sustainability

MDPI

Article

Magnetic Fe_3O_4-Ag^0 Nanocomposites for Effective Mercury Removal from Water

Vassilis J. Inglezakis [1], Aliya Kurbanova [2], Anara Molkenova [3], Antonis A. Zorpas [4,*] and Timur Sh. Atabaev [3,*]

1 Environmental Science & Technology Group (ESTg), Department of Chemical &Materials Engineering, Nazarbayev University, Nur-Sultan 010000, Kazakhstan; vasileios.inglezakis@nu.edu.kz
2 The Environment & Resource Efficiency Cluster (EREC), Nazarbayev University, Nur-Sultan 010000, Kazakhstan; aliya.kurbanova@nu.edu.kz
3 Department of Chemistry, Nazarbayev University, Nur-Sultan 010000, Kazakhstan; anara.molkenova@nu.edu.kz
4 Lab of Chemical Engineering & Engineering Sustainability, Faculty of Pure & Applied Science, Open University of Cyprus, GiannouKranidioti 33, Nicosia 2220, Cyprus
* Correspondence: antonis.zorpas@ouc.ac.cy (A.A.Z.); timur.atabaev@nu.edu.kz (T.S.A.); Tel.: +357-224-119-36 (A.A.Z.)

Received: 12 May 2020; Accepted: 23 June 2020; Published: 7 July 2020

Abstract: In this study, magnetic Fe_3O_4 particles and Fe_3O_4-Ag^0 nanocomposites were prepared by a facile and green method, fully characterized and used for the removal of Hg^{2+} from water. Characterizations showed that the Fe_3O_4 particles are quasi-spherical with an average diameter of 217 nm and metallic silver nanoparticles formed on the surface with a size of 23–41 nm. The initial Hg^{2+} removal rate was very fast followed by a slow increase and the maximum solid phase loading was 71.3 mg/g for the Fe_3O_4-Ag^0 and 28 mg/g for the bare Fe_3O_4. The removal mechanism is complex, involving Hg^{2+} adsorption and reduction, Fe^{2+} and Ag^0 oxidation accompanied with reactions of Cl^- with Hg^+ and Ag^+. The facile and green synthesis process, the fast kinetics and high removal capacity and the possibility of magnetic separation make Fe_3O_4-Ag^0 nanocomposites attractive materials for the removal of Hg^{2+} from water.

Keywords: nanocomposites; magnetite; silver; mercury; amalgamation

1. Introduction

Mercury and its compounds are considered to be extremely hazardous pollutants. Contamination of the environment with mercury has become a global problem and mercury polluted areas have been identified worldwide [1]. In most cases, the release of Hg^0 or Hg^{2+} into the environment occurs due to industrial emissions, transportation, waste treatment or technological accidents [2]. Therefore, the development of efficient methods for the removal of mercury from water is imperative. Several removal and immobilization methods are available, such as membrane separation, reduction, precipitation, physical and chemical adsorption, ion exchange and bioremediation [3,4]. Of these methods, adsorption exhibits several advantages in terms of process design, operation and cost and it is the most studied one [4]. A number of materials have been used as adsorbents for the removal of Hg^{2+} from water, including activated carbons [5], zeolites [6,7], resins and other polymers [8–11] and silver-modified materials [7,12,13].

Silver is an important metal that can form various amalgam compounds with mercury such as AgHg, Ag_2Hg_3, Ag_3Hg_4, Ag_4Hg_5 and $Ag_{10}Hg_{13}$ [14]. The amalgamation reaction can be greatly enhanced by utilizing Ag in the form of nanocomposites. Such nanocomposites based on silica,

magnetite, titanium oxide and alumina have been studied for the removal of heavy metals and mercury from water [15–19]. Among them, magnetite-based nanocomposites are being broadly studied for use in water purification owing to their low cost, simple application, and absence of toxicity towards the environment [20,21]. Furthermore, magnetite nanoparticles are easily separable from the aqueous solution when a magnetic field is applied and can be reused several times [22]. Heavy metals can be bound to the surface of magnetite by complexation, precipitation and adsorption mechanisms. Various types of magnetic nanomaterials are being investigated for the extraction of hazardous pollutants from water. In particular, magnetite-based nanocomposites show high efficiency in the removal and recovery of copper, zinc, nickel and mercury ions from industrial wastewater [23,24].

Fe_3O_4@SiO_2 magnetic nanoparticles modified by grafting poly(1-vinylimidazole) oligomer were used to remove Hg^{2+} from water reaching a maximum capacity of 346 mg/g [21]. Fe_3O_4 nanoparticles coated with silica shells functionalized with dithiocarbamate groups were used for mercury removal from seawater and quantification of mercury in natural waters [25,26]. Nanocomposites based on Fe_3O_4 nanoparticles, chitosan nanoparticles and polythiophene were used for Hg^{2+} removal from aqueous solutions reaching a loading of about 50 mg/g [27]. Thiol-functionalized Fe_3O_4 nanoparticles have shown a high removal capacity for Hg^{2+} reaching 345 mg/g [28]. Fe_3O_4 nanoparticles coated with amino organic ligands and yam peel biomass reached a loading of about 60 mg/g [29]. Dithiothreitol functionalized Fe_3O_4 nanoparticles showed a capacity of 6.3 mg/g and activated carbon doped with Fe_3O_4 nanoparticles reached a capacity of 38.3 mg/g [30]. Dithiocarbamate surface functionalized Fe_3O_4 particles reached a loading of 122–246 mg/g [31]. Zeolite-magnetite composites were used to remove Hg^{2+} from water reaching a maximum loading of 26.2 mg/g [32]. Fe_3O_4 particles have been also used as core covered with a silica shell [33,34].

As the literature review demonstrates the direct surface interactions of mercury ions with bare Fe_3O_4 and Fe_3O_4-Ag^0 nanocompositeshave not been studied so far. An exception is the work of Dong et al. [35] who used Fe_3O_4-Ag^0 particles but for the removal of Hg^0 from flue gas. On the synthesis part, great attention is paid to the development of green processes with minimal use of toxic substances [36]. Plant extracts utilization as reducing and stabilizing agents have drawn considerable attention for the synthesis of metallic nanoparticles as it is considered an eco-friendly method [37,38]. Furthermore, the synthesis process should be low-cost and easily scalable for mass production. Such a green synthesis of Ag nanoparticles on magnetic iron oxide modified by a herbal tea extract has been studied for antibacterial activity and 4-nitrophenol reduction [37]. In this study, we synthesized magnetic Fe_3O_4-Ag^0 nanocomposites by a facile method using green tea extract. The nanocomposite was then used as a magnetically separable adsorbent for efficient mercury removal from water. The mechanism of mercury removal is discussed in detail and verified by advanced characterization methods.

2. Materials and Methods

2.1. Chemicals

High purity iron (III) chloride hexahydrate ($FeCl_3{\cdot}6H_2O$, 99%), anhydrous sodium acetate (CH_3COONa, 99.0%), anhydrous ethylene glycol ($C_2H_6O_2$, 99.8%), silver nitrate ($AgNO_3$, ≥99%), mercury (II) chloride ($HgCl_2$, 99.8%) were used as received. Green tea was purchased at the local market.

2.2. Synthesis of Fe_3O_4

Magnetite particles were synthesized according to previously published protocols [39,40]. In a typical synthesis process, $FeCl_3{\cdot}6H_2O$ (2.16 g) and CH_3COONa (6 g) were dissolved in 15mL ethylene glycol. The prepared mixture solution was then transferred to a Teflon-lined stainless-steel autoclave and then heated at 200 °C for 8 h, with heating rate of 10 °C per 1 min. The black product was washed by magnet decantation several times with water/ethanol and then dried at 40 °C. 2.3. Synthesis of Fe_3O_4-Ag^0.

Green tea extract (GTE) was prepared by boiling 0.2 g of dried green tea leaves in 20 mL of water for 5 min. The GTE was then filtered using a Whatman filter paper N1 to obtain an aqueous extract of green tea. To prepare the Fe_3O_4-Ag^0 nanocomposites, 100 mg of magnetite spheres were dispersed in 10 mL of water and dispersed for 20 min. To the above solution, 500 µL of GTE was added and the solution was stirred at room temperature for 24 h. Finally, $AgNO_3$ (20 mg) was added to the solution and kept under stirring for 24 h. The as-prepared composite was separated by the magnet, washed with water/ethanol and then dried at 30 °C.

2.3. Mercury Removal Efficiency

The Hg^{2+} removal efficiency of Fe_3O_4 particles and Fe_3O_4-Ag^0 nanocomposites was studied in $HgCl_2$ solutions. A stock solution of Hg^{2+} (100 and 200 ppm) was prepared by dissolving $HgCl_2$ in deionized water. The Hg^{2+} solution volume was 20 mL and the solids mass 50 mg. All adsorption experiments were performed without any stirring at room temperature (23 ± 2 °C) without pH adjustment. The mercury concentration in the solutions was measured by a mercury analyzer (Lumex RA-915M) until no concentration changes were observed, i.e., until equilibrium was attained. All experiments were performed in duplicate and the average standard deviation was 2%.

2.4. Characterization

The crystalline phase and the structure of the synthesized Fe_3O_4 particles and Fe_3O_4-Ag^0 nanocomposites before and after mercury adsorption were performed using an X-ray diffractometer (XRD) (RigakuSmartLab, Tokyo, Japan). The surface of the materials was studied by Scanning Electron Microscopy (SEM) using a Zeiss Auriga Crossbeam 540. Chemical analysis was carried out using an Energy-Dispersive X-ray spectrometer (Aztec, Oxford Instruments, Abingdon, UK). The nanoscale analysis was done with a high-resolution JEOL JEM-1400 Plus transmission electron microscope (TEM), operating at 120 kV.

2.5. Calculations

The kinetics of mercury removal from water was studied in order to obtain information about the adsorption mechanism of the pure Fe_3O_4 particles and Fe_3O_4-Ag^0 nanocomposites. The percentage of mercury removal (R) was calculated using as follows:

$$R\ (\%) = ((C_i - C_f)/C_i) \times 100 \quad (1)$$

$$q\ (mg/g) = (C_i - C_f) \times V/m \quad (2)$$

where C_i and C_f (mg/L) are the initial and final concentrations of Hg^{2+}, V (L) is the volume of the solution and m (g) is mass of the adsorbent.

3. Results and Discussion

SEM analysis was used to investigate the morphology of as-prepared bare Fe_3O_4 particles and Fe_3O_4-Ag^0 nanocomposites. Figure 1A shows that the bare Fe_3O_4 particles were quasi-spherical and had a mean diameter of 217 ± 76 nm. Figure 1B shows that the surface of the Fe_3O_4-Ag^0 nanocomposites became rougher because of Ag nanoparticle (23–41 nm) deposition on the surface of the Fe_3O_4 particles. The TEM image (Figure 1C) and EDX analysis (Figure 1D) confirmed that Fe_3O_4 particles were decorated with Ag nanoparticles. In particular, main elements such as Fe, O and Ag were clearly detectable in the EDX spectrum of Fe_3O_4-Ag^0 nanocomposites. Figure 1E shows that Fe_3O_4-Ag^0 nanocompositesweremagnetic and could be conveniently extracted by the use of a permanent magnet.

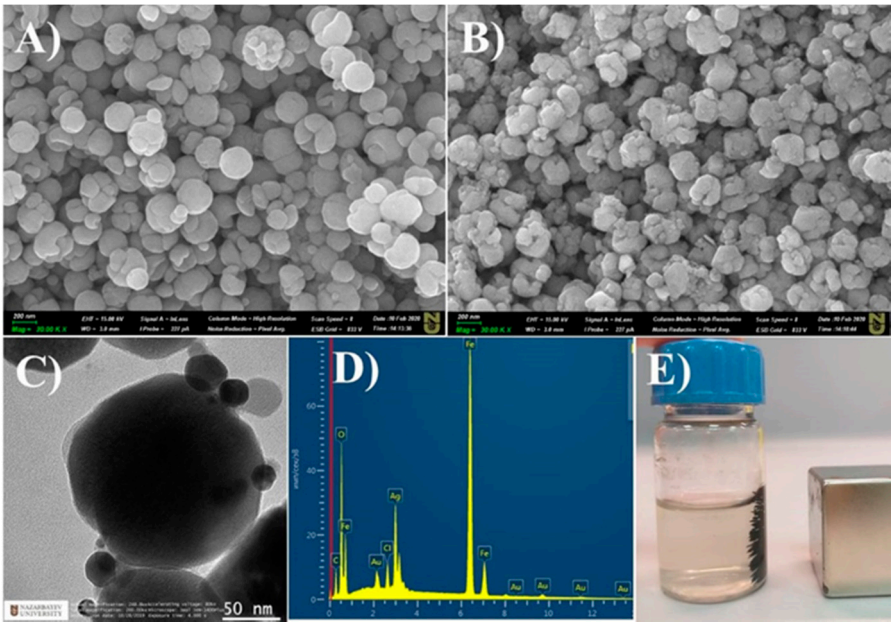

Figure 1. SEM images of (**A**) bareFe_3O_4 and (**B**) Fe_3O_4-Ag^0 particles. TEM image (**C**) of an individual Fe_3O_4-Ag^0 particle, (**D**) EDX spectrum and (**E**) digital image of Fe_3O_4-Ag^0 particles in a water solution attracted by a permanent magnet.

XRD analysis of the bare Fe_3O_4 and Fe_3O_4-Ag^0 confirmed the successful deposition of Ag nanoparticles on the surface of Fe_3O_4 particles. Figure 2 shows that diffraction peaks at 30.1°, 35.5°, 43.1°, 53.7°, 57.3° and 62.6° couldbe indexed to the (220), (311), (400), (422), (511) and (440) planes of the face-centered cubic structure of the Fe_3O_4(JCPDS # 19-629) and the four peaks located at 38.2°, 44.3°, 64.2° and 73.9° corresponded to the characteristic (111), (200), (220) and (311) reflection planes of the face-centered cubic Ag (JCPDS # 04-0783). It should be noted that the strong diffraction peaks indicated the formation of particles with good crystallinity and purity since no other peaks were detected.

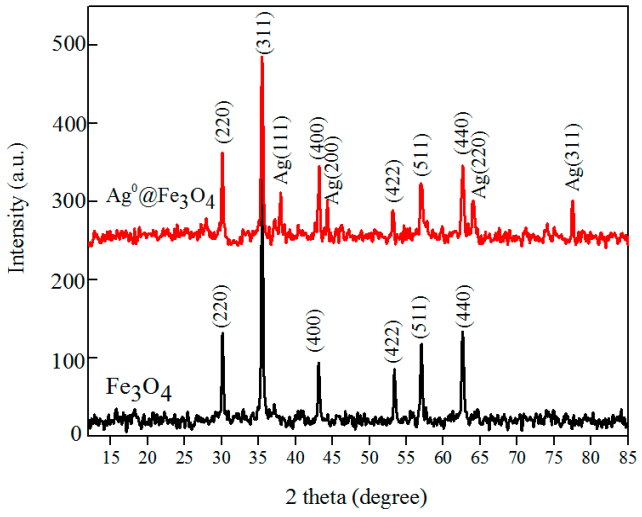

Figure 2. XRD patterns of bare Fe_3O_4 and Fe_3O_4-Ag^0 particles.

Figure 3A shows the adsorption kinetics results. It was found that Fe_3O_4-Ag^0 removed more than 80% of the mercury within the first hour followed by a slow approach to an equilibrium point with a maximum solid phase loading of 71.3 mg/g. On the other hand, the bare Fe_3O_4 removed less than 10% of mercury after the first hour and less than 40% at equilibrium, reaching a solid phase loading of

about 28 mg/g. Qualitatively similar trends were observed for the removal of Hg^0 from flue gas by using bare Fe_3O_4 and Fe_3O_4-Ag^0 [35]. Some studies argue that magnetite either does not remove Hg^{2+} or removes only up to 1.14 mg/g [21,41]. As mentioned in the introduction, there are no studies on the removal of Hg^{2+} from water by the use of this material and for comparison representative published studies are presented in Table 1. As is evident, capacity depends on the materials and conditions used. An important advantage of Fe_3O_4-Ag^0 is the ease of separation of the solid phase after the adsorption process.

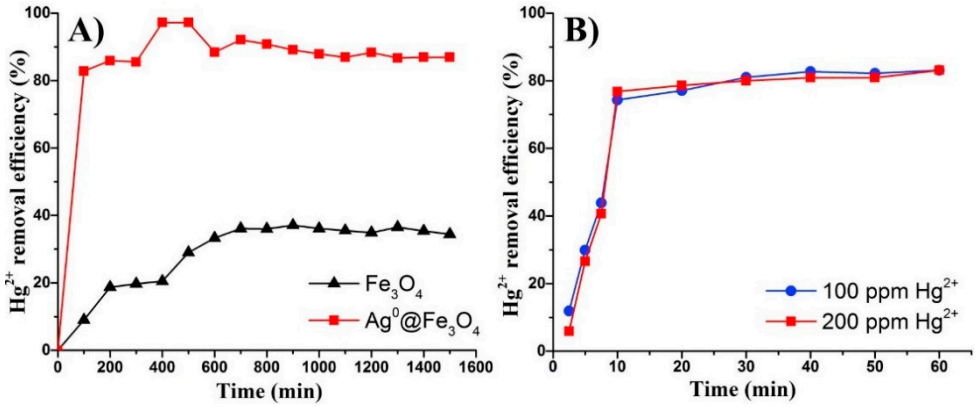

Figure 3. Hg^{2+} removal efficiency using bare Fe_3O_4 and Fe_3O_4-Ag^0 at 100 ppm (**A**) and the comparison between 100 and 200 ppm for Fe_3O_4-Ag^0 (**B**).

Table 1. Published studies on the removal of mercury from aqueous solutions.

Material	Capacity (mg/g)	Reference
Dithiothreitol functionalized Fe_3O_4 nanoparticles	6.3	[30]
SiO_2-Ag^0 nanocomposites	7.8–8.3	[19]
Synthetic zeolites	20.5–22.3	[42]
Zeolite-magnetite composites	26.2	[32]
Activated carbon doped with Fe_3O_4 nanoparticles	38.3	[30]
Nanocomposites based on Fe_3O_4 nanoparticles, chitosan nanoparticles and polythiophene	50	[27]
Fe_3O_4 nanoparticles coated with amino organic ligands and yam peel biomass	60	[29]
Dithiocarbamate surface functionalized Fe_3O_4 particles	122–246	[31]
Mesoporous silica-ammonium (4-chloro-2-mercaptophenyl) carbamodithioate	164	[43]
Thiol-functionalized Fe_3O_4 nanoparticles	345	[28]
Fe_3O_4@SiO_2 magnetic nanoparticles modified by grafting poly(1-vinylimidazole)	346	[21]
Cryogels	240–742	[11]

Additional experiments for short time demonstrated that reaction on the surface of Fe_3O_4-Ag^0 particles was rapid and the majority of mercury ions are removed within the first 10 min (Figure 3B). Almost the same trend was observed for two different concentrations of Hg^{2+}.

The interaction of Hg^{2+} with bare Fe_3O_4 and Fe_3O_4-Ag^0 was further investigated using SEM, EDX and XRD. Figure 4A shows the SEM analysis of the bare Fe_3O_4 after contact with Hg^{2+} for 12 h. It was clear that the Fe_3O_4 particles still retained the quasi-spherical shape. An EDX survey (Figure 4B) revealed that a small quantity of Hg and Cl were adsorbed on the surface of Fe_3O_4 particles. Analysis of the Fe_3O_4-Ag^0 after contact with Hg^{2+} for 12 h was also performed for comparison. Figure 5A shows that the morphology of the Fe_3O_4-Ag^0 particles was not changed significantly. However, EDX analysis revealed that the quantity of adsorbed Hg and Cl significantly increased. The detected amount of Hg

(wt.%) became five times higher, while the detected amount of Cl (wt.%) became eight times higher. These results demonstrated that the addition of Ag^0wasbeneficial in terms of Hg^{2+} removal.

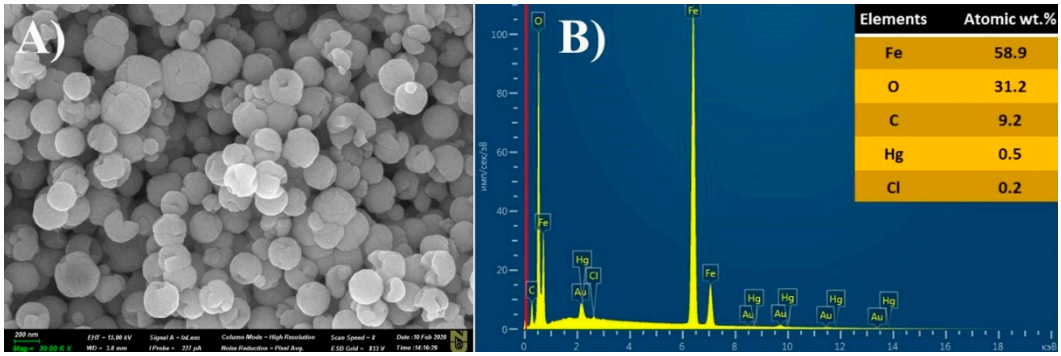

Figure 4. SEM image (**A**) and EDX survey (**B**) of bare Fe_3O_4 after contact with Hg^{2+} for 12 h.

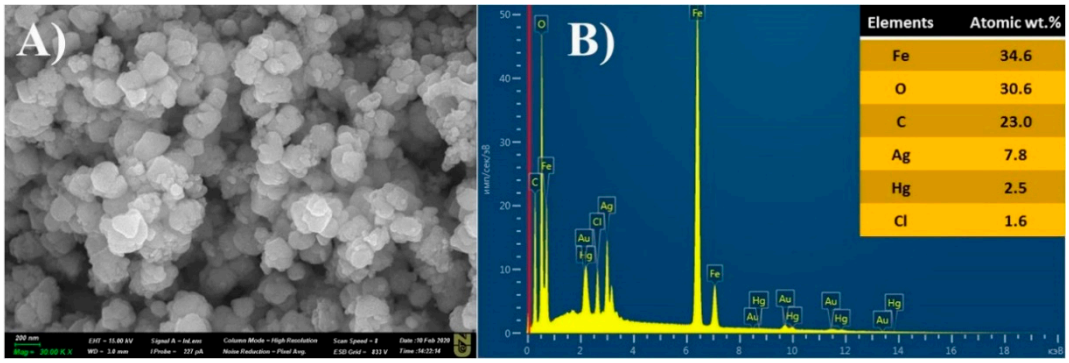

Figure 5. SEM image (**A**) and EDX survey (**B**) of Fe_3O_4-Ag^0 after contact with Hg^{2+} for 12 h.

An XRD analysis was performed to elucidate the adsorption pathways on the surface of bare Fe_3O_4 and Fe_3O_4-Ag^0 (Figure 6). Upon contact of Fe_3O_4 particles with Hg^{2+}, new peaks at 24° and 32° appeared due to the formation of HgO [44] and a peak at 44° appeared due to the formation of Hg_2Cl_2 [45]. The reaction mechanism between mercury and magnetite is still not well understood. However, a recent report suggested that Hg^{2+}couldbe adsorbed on the surface of magnetite from a $HgCl_2$ solution and then reduced to volatile Hg^0 by Fe^{2+} [46]. The formation of volatile Hg^0 is difficult to confirm but if it happens it obviously gives no trace on the XRD. Another study on magnetite found that in the absence of chloride ions, Hg^{2+} is reduced to Hg^0, while in the presence of chloride ions it is reduced to Hg^+ resulting in Hg_2Cl_2 [47], which is in agreement with the results of the present study.The interaction of Fe species with Hg^{2+} and the redox reactions resulting in Hg_2Cl_2, Hg^0 and HgO are discussed in other studies as well [41]. The possible reactions are the following:

$$2Fe^{2+} + Hg^{2+} \rightarrow 2Fe^{3+} + Hg^0 \quad (3)$$

$$Fe^{2+} + Hg^{2+} \rightarrow Fe^{3+} + Hg^+ \quad (4)$$

$$Hg^{2+} + 0.5O_2 \rightarrow HgO \quad (5)$$

$$2Hg^+ + 2Cl^- \rightarrow Hg_2Cl_2 \quad (6)$$

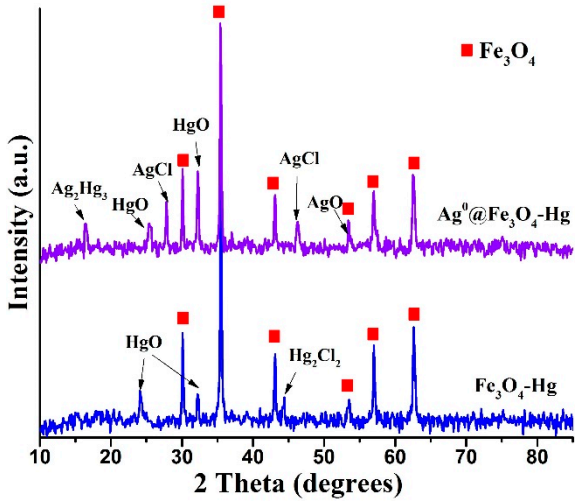

Figure 6. XRD patterns of Fe_3O_4 and Fe_3O_4-Ag^0 after 12 h contact with $HgCl_2$ solution.

In the case of Fe_3O_4-Ag^0 nanocomposites, the appearance of a new peak at around 17° probably indicated the formation of an Hg-Ag amalgam (moschellandbergite phase, Ag_2Hg_3) [48]. The absence of literature on the removal of Hg^{2+} from aqueous solutions by the use of Fe_3O_4-Ag^0 nanocomposites is difficult to support this conclusion. However, there are papers presenting the removal of Hg from a gas phase by the use of Fe_3O_4-Ag^0 nanocomposites [35] where the formation of Hg-Ag amalgams is offered as the best explanation for the efficiency of the nanocomposite in comparison to the bare magnetite. Additional peaks at around 27° and 46° were indexed to the AgCl [49] structure, which appeared due to the reaction between the Ag^+ and Cl^-. Furthermore, a peak at 53° appeared due to the formation of monoclinic AgO [50]. The formation of Ag_2Hg_3 and Hg_2Cl_2 and the effect of Hg^{2+} speciation on the reaction mechanismsare discussed in more detail on different Ag^0 nanocomposites elsewhere [19,42]. Thus, in addition to reactions (3)–(6), in the presence of Ag^0 the following reactions can occur:

$$2Ag^0 + Hg^{2+} \rightarrow 2Ag^+ + Hg^0 \quad (7)$$

$$Ag^0 + Hg^{2+} \rightarrow Ag^+ + Hg^+ \quad (8)$$

$$Ag^0 + 0.5O_2 \rightarrow AgO \quad (9)$$

$$Ag^+ + Cl^- \rightarrow AgCl \quad (10)$$

$$2Ag^0 + 3Hg^0 \rightarrow Ag_2Hg_3 \quad (11)$$

The results suggest that the interactions on the surface of Fe_3O_4 and Fe_3O_4-Ag^0 are complex and there is a competition between several reactions, which govern the removal rate of Hg^{2+} from water. As it is clear, XPS analysis should be conducted in order to further investigate the possible redox reactions.

4. Conclusions

Fe_3O_4 particles and Fe_3O_4-Ag^0 nanocomposites were successfully synthesized, characterized and used for the removal of Hg^{2+} from water. The results showed that micron-sized magnetite particles are formed on which Ag^0 nanoparticles are anchored. The mercury removal experiments showed that Fe_3O_4-Ag^0 nanocomposites are more effective than Fe_3O_4 particles. XRD analysis revealed the formation of several compounds on the surface of the materials, including HgO, Hg_2Cl_2, AgCl, AgO and possibly Ag_2Hg_3. The formation of these compounds is a strong indication of surface redox reactions between Fe^{2+}, O_2, Ag^0 and Hg^{2+}. Thus, several reactions can occur at the same time and further characterizations, such as XPS, are needed in order to draw safe conclusions. The facile synthesis,

the fast removal and the magnetic properties render the Fe_3O_4-Ag^0 nanocomposite a promising material for Hg^{2+} removal from water.

Author Contributions: V.J.I., conceptualization, methodology, validation, writing—review and editing, supervision, project administration, A.K., methodology, data curation, writing—original draft preparation, A.M., writing—review and editing, A.A.Z., data curation, validation, writing—review and editing T.S.A., conceptualization, methodology, validation, writing—review and editing. All authors have read and agreed to the published version of the manuscript.

Funding: This research was funded by Nazarbayev University Grant Number 110119FD4536 and the APC was funded by the same project.

Acknowledgments: The authors wish to thank the operators of Nazarbayev University Core Facilities for their help.

Conflicts of Interest: The authors declare no conflict of interest.

References

1. Budnik, L.T.; Casteleyn, L. Mercury pollution in modern times and its socio-medical consequences. *Sci. Total Environ.* **2019**, *654*, 720–734. [CrossRef] [PubMed]
2. Driscoll, C.T.; Mason, R.P.; Chan, H.M.; Jacob, D.J.; Pirrone, N. Mercury as a global pollutant: Sources, pathways, and effects. *Environ. Sci. Technol.* **2013**, *47*, 4967–4983. [CrossRef]
3. Azimi, A.; Azari, A.; Rezakazemi, M.; Ansarpour, M. Removal of Heavy Metals from Industrial Wastewaters: A Review. *ChemBioEng Rev.* **2017**, *4*, 37–59. [CrossRef]
4. Wang, L.; Hou, D.; Cao, Y.; Ok, Y.S.; Tack, F.M.G.G.; Rinklebe, J.; O'Connor, D. Remediation of mercury contaminated soil, water, and air: A review of emerging materials and innovative technologies. *Environ. Int.* **2020**, *134*, 105281. [CrossRef] [PubMed]
5. Saha, D.; Barakat, S.; Van Bramer, S.E.; Nelson, K.A.; Hensley, D.K.; Chen, J. Noncompetitive and Competitive Adsorption of Heavy Metals in Sulfur-Functionalized Ordered Mesoporous Carbon. *ACS Appl. Mater. Interfaces* **2016**, *8*, 34132–34142. [CrossRef] [PubMed]
6. Tauanov, Z.; Tsakiridis, P.E.; Shah, D.; Inglezakis, V.J. Synthetic sodalite doped with silver nanoparticles: Characterization and mercury (II) removal from aqueous solutions. *J. Environ. Sci. Health A Toxic/Hazard. Subst. Environ. Eng.* **2019**, *54*, 951–959. [CrossRef] [PubMed]
7. Tauanov, Z.; Tsakiridis, P.E.; Mikhalovsky, S.V.; Inglezakis, V.J. Synthetic coal fly ash-derived zeolites doped with silver nanoparticles for mercury (II) removal from water. *J. Environ. Manag.* **2018**, *224*, 164–171. [CrossRef]
8. De Clercq, J. Removal of mercury from aqueous solutions by adsorption on a new ultra stable mesoporous adsorbent and on a commercial ion exchange resin. *Int. J. Ind. Chem.* **2012**, *3*, 1. [CrossRef]
9. Ge, H.; Hua, T. Synthesis and characterization of poly(maleic acid)-grafted crosslinked chitosan nanomaterial with high uptake and selectivity for Hg(II) sorption. *Carbohydr. Polym.* **2016**, *153*, 246–252. [CrossRef]
10. Wang, X.; Yang, L.; Zhang, J.; Wang, C.; Li, Q. Preparation and characterization of chitosan–poly(vinyl alcohol)/bentonite nanocomposites for adsorption of Hg(II) ions. *Chem. Eng. J.* **2014**, *251*, 404–412. [CrossRef]
11. Baimenov, A.Z.; Berillo, D.A.; Moustakas, K.; Inglezakis, V.J. Efficient removal of mercury (II) from water by use of cryogels and comparison to commercial adsorbents under environmentally relevant conditions. *J. Hazard. Mater.* **2020**, *399*, 123056. [CrossRef] [PubMed]
12. Sumesh, E.; Bootharaju, M.S.; Anshup; Pradeep, T. A practical silver nanoparticle-based adsorbent for the removal of Hg^{2+} from water. *J. Hazard. Mater.* **2011**, *189*, 450–457. [CrossRef]
13. Qu, Z.; Fang, L.; Chen, D.; Xu, H.; Yan, N. Effective and regenerable Ag/graphene adsorbent for Hg(II) removal from aqueous solution. *Fuel* **2017**, *203*, 128–134. [CrossRef]
14. Gumiński, C. Review Selected properties of simple amalgams. *J. Mater. Sci.* **1989**, *24*, 2661–2676. [CrossRef]
15. Song, B.Y.; Eom, Y.; Lee, T.G. Removal and recovery of mercury from aqueous solution using magnetic silica nanocomposites. *Appl. Surf. Sci.* **2011**, *257*, 4754–4759. [CrossRef]
16. Behjati, M.; Baghdadi, M.; Karbassi, A. Removal of mercury from contaminated saline wasters using dithiocarbamate functionalized-magnetic nanocomposite. *J. Environ. Manag.* **2018**, *213*, 66–78. [CrossRef]
17. Dou, B.; Dupont, V.; Pan, W.; Chen, B. Removal of aqueous toxic Hg(II) by synthesized TiO_2 nanoparticles and TiO_2/montmorillonite. *Chem. Eng. J.* **2011**, *166*, 631–638. [CrossRef]

18. Wang, X.; Zhan, C.; Kong, B.; Zhu, X.; Liu, J.; Xu, W.; Cai, W.; Wang, H. Self-curled coral-like γ-Al_2O_3 nanoplates for use as an adsorbent. *J. Colloid Interface Sci.* **2015**, *453*, 244–251. [CrossRef]
19. Azat, S.; Arkhangelsky, E.; Papathanasiou, T.; Zorpas, A.A.; Abirov, A.; Inglezakis, V.J. Synthesis of biosourced silica-Ag nanocomposites and amalgamation reaction with mercury in aqueous solutions. *Comptes Rendus Chim.* **2020**, *23*, 77–92. [CrossRef]
20. Gong, Y.; Huang, Y.; Wang, M.; Liu, F.; Zhang, T. Application of Iron-Based Materials for Remediation of Mercury in Water and Soil. *Bull. Environ. Contam. Toxicol.* **2019**, *102*, 721–729. [CrossRef]
21. Shan, C.; Ma, Z.; Tong, M.; Ni, J. Removal of Hg(II) by poly(1-vinylimidazole)-grafted Fe_3O_4 at SiO_2 magnetic nanoparticles. *Water Res.* **2015**, *69*, 252–260. [CrossRef] [PubMed]
22. Kumari, M.; Pittman, C.U.; Mohan, D. Heavy metals [chromium (VI) and lead (II)] removal from water using mesoporous magnetite (Fe_3O_4) nanospheres. *J. Colloid Interface Sci.* **2015**, *442*, 120–132. [CrossRef] [PubMed]
23. Yang, J.; Hou, B.; Wang, J.; Tian, B.; Bi, J.; Wang, N.; Li, X.; Huang, X. Nanomaterials for the removal of heavy metals from wastewater. *Nanomaterials* **2019**, *9*, 424. [CrossRef] [PubMed]
24. Horst, M.F.; Lassalle, V.; Ferreira, M.L. Nanosized magnetite in low cost materials for remediation of water polluted with toxic metals, azo- and antraquinonic dyes. *Front. Environ. Sci. Eng.* **2015**, *9*, 746–769. [CrossRef]
25. Tavares, D.S.; Vale, C.; Lopes, C.B.; Trindade, T.; Pereira, E. Reliable quantification of mercury in natural waters using surface modified magnetite nanoparticles. *Chemosphere* **2019**, *220*, 565–573. [CrossRef] [PubMed]
26. Mohmood, I.; Lopes, C.B.; Lopes, I.; Tavares, D.S.; Soares, A.M.V.M.; Duarte, A.C.; Trindade, T.; Ahmad, I.; Pereira, E. Remediation of mercury contaminated saltwater with functionalized silica coated magnetite nanoparticles. *Sci. Total Environ.* **2016**, *557–558*, 712–721. [CrossRef]
27. Morsi, R.E.; Al-Sabagh, A.M.; Moustafa, Y.M.; ElKholy, S.G.; Sayed, M.S. Polythiophene modified chitosan/magnetite nanocomposites for heavy metals and selective mercury removal. *Egypt. J. Pet.* **2018**, *27*, 1077–1085. [CrossRef]
28. Oveisi, F.; Nikazar, M.; Razzaghi, M.H.; Mirrahimi, M.A.S.; Jafarzadeh, M.T. Effective removal of mercury from aqueous solution using thiol-functionalized magnetic nanoparticles. *Environ. Nanotechnol. Monit. Manag.* **2017**, *7*, 130–138. [CrossRef]
29. Marimón-Bolívar, W.; Tejeda-Benítez, L.; Herrera, A.P. Removal of mercury (II) from water using magnetic nanoparticles coated with amino organic ligands and yam peel biomass. *Environ. Nanotechnol. Monit. Manag.* **2018**, *10*, 486–493. [CrossRef]
30. Okamoto, T.; Tachibana, S.; Miura, O.; Takeuchi, M. Mercury removal from solution by superconducting magnetic separation with nanostructured magnetic adsorbents. *Phys. C Supercond. Its Appl.* **2011**, *471*, 1516–1519. [CrossRef]
31. Figueira, P.; Lopes, C.B.; Daniel-da-Silva, A.L.; Pereira, E.; Duarte, A.C.; Trindade, T. Removal of mercury (II) by dithiocarbamate surface functionalized magnetite particles: Application to synthetic and natural spiked waters. *Water Res.* **2011**, *45*, 5773–5784. [CrossRef]
32. Andrade, Â.L.; Cavalcante, L.C.D.; Fabris, J.D.; Pereira, M.C.; Ardisson, J.D.; Pizarro, C. Zeolite-magnetite composites to remove Hg^{2+} from water. *Hyperfine Interact.* **2019**, *240*, 18–23. [CrossRef]
33. Girginova, P.I.; Daniel-da-Silva, A.L.; Lopes, C.B.; Figueira, P.; Otero, M.; Amaral, V.S.; Pereira, E.; Trindade, T. Silica coated magnetite particles for magnetic removal of Hg^{2+} from water. *J. Colloid Interface Sci.* **2010**, *345*, 234–240. [CrossRef] [PubMed]
34. Dong, J.; Xu, Z.; Wang, F. Engineering and characterization of mesoporous silica-coated magnetic particles for mercury removal from industrial effluents. *Appl. Surf. Sci.* **2008**, *254*, 3522–3530. [CrossRef]
35. Dong, L.; Xie, J.; Fan, G.; Huang, Y.; Zhou, J.; Sun, Q.; Wang, L.; Guan, Z.; Jiang, D.; Wang, Y. Experimental and theoretical analysis of element mercury adsorption on Fe_3O_4/Ag composites. *Korean J. Chem. Eng.* **2017**, *34*, 2861–2869. [CrossRef]
36. Marimon-Bolivar, W.; Toussaint-Jimenez, N. A review on green synthesis of magnetic nanoparticles (magnetite) for environmental applications. In Proceedings of the 2019 Congreso Internacional de Innovación y Tendencias en Ingenieria (CONIITI), Bogotá, Colombia, 2–4 October 2019.
37. Shahriary, M.; Veisi, H.; Hekmati, M.; Hemmati, S. In situ green synthesis of Ag nanoparticles on herbal tea extract (Stachys lavandulifolia)-modified magnetic iron oxide nanoparticles as antibacterial agent and their 4-nitrophenol catalytic reduction activity. *Mater. Sci. Eng. C* **2018**, *90*, 57–66. [CrossRef]
38. Chrysochoou, M.; Oakes, J.; Dyar, M.D. Investigation of iron reduction by green tea polyphenols. *Appl. Geochem.* **2018**, *97*, 263–269. [CrossRef]

39. Madrid, S.I.U.; Pal, U.; Jesus, F.S.-D. Controlling size and magnetic properties of Fe_3O_4 clusters in solvothermal process. *Adv. Nano Res.* **2014**, *2*, 187–198. [CrossRef]
40. Sun, D.D.; Zhang, J.; Sun, D.D. Solvothermal synthesis and magnetic properties of Fe_3O_4 microspheres. *Adv. Mater. Res.* **2012**, *393–395*, 947–950.
41. Ganguly, M.; Dib, S.; Ariya, P.A. Fast, Cost-effective and Energy Efficient Mercury Removal-Recycling Technology. *Sci. Rep.* **2018**, *8*, 16255. [CrossRef]
42. Tauanov, Z.; Lee, J.; Inglezakis, V.J. Mercury reduction and chemisorption on the surface of synthetic zeolite silver nanocomposites: Equilibrium studies and mechanisms. *J. Mol. Liq.* **2020**, *305*, 112825. [CrossRef]
43. Awual, M.R.; Hasan, M.M.; Eldesoky, G.E.; Khaleque, M.A.; Rahman, M.M.; Naushad, M. Facile mercury detection and removal from aqueous media involving ligand impregnated conjugate nanomaterials. *Chem. Eng. J.* **2016**, *290*, 243–251. [CrossRef]
44. Abdelrahman, E.A.; Hegazey, R.M. Facile Synthesis of HgO Nanoparticles Using Hydrothermal Method for Efficient Photocatalytic Degradation of Crystal Violet Dye Under UV and Sunlight Irradiation. *J. Inorg. Organomet. Polym. Mater.* **2019**, *29*, 346–358. [CrossRef]
45. Fedoseeva, Y.V.; Orekhov, A.S.; Chekhova, G.N.; Koroteev, V.O.; Kanygin, M.A.; Senkovskiy, B.V.; Chuvilin, A.; Pontiroli, D.; Riccò, M.; Bulusheva, L.G.; et al. Single-Walled Carbon Nanotube Reactor for Redox Transformation of Mercury Dichloride. *ACS Nano* **2017**, *11*, 8643–8649. [CrossRef] [PubMed]
46. Wiatrowski, H.A.; Das, S.; Kukkadapu, R.; Ilton, E.S.; Barkay, T.; Yee, N. Reduction of Hg(II) to Hg(0) by magnetite. *Environ. Sci. Technol.* **2009**, *43*, 5307–5313. [CrossRef]
47. Pasakarnis, T.S.; Boyanov, M.I.; Kemner, K.M.; Mishra, B.; O'Loughlin, E.J.; Parkin, G.; Scherer, M.M. Influence of chloride and Fe(II) content on the reduction of Hg(II) by magnetite. *Environ. Sci. Technol.* **2013**, *47*, 6987–6994. [CrossRef]
48. Harika, V.K.; Kumar, V.B.; Gedanken, A. One-pot Sonochemical Synthesis of Hg–Ag Alloy Microspheres from Liquid Mercury. *Ultrason. Sonochem.* **2018**, *40*, 157–165. [CrossRef]
49. Zhu, M.; Chen, P.; Liu, M. Sunlight-driven plasmonic photocatalysts based on Ag/AgCl nanostructures synthesized via an oil-in-water medium: Enhanced catalytic performance by morphology selection. *J. Mater. Chem.* **2011**, *21*, 16413–16419. [CrossRef]
50. Zhang, R.; Zhang, D.; Mao, H.; Song, W.; Gao, G.; Liu, F. Preparation and characterization of Ag/AgO nanoshells on carboxylated polystyrene latex particles. *J. Mater. Res.* **2006**, *21*, 349–354. [CrossRef]